Supporting Information

Targeted Control over Porosities and Functionalities of Conjugated Microporous Polycarbazole Networks for CO_2-Selective Capture and H_2 Storage

Yaozu Liao,[*,†,‡] *Zhonghua Cheng,*[†] *Matthias Trunk,*[‡] *Arne Thomas,*[*,‡]

[†] State Key Laboratory for Modification of Chemical Fibers and Polymer Materials, College of Materials Science and Engineering, Donghua University, Shanghai 201620, China

[‡] Department of Chemistry, Functional Materials, Technische Universität Berlin, Berlin 10623, Germany

Corresponding Authors: yzliao@dhu.edu.cn, arne.thomas@tu-berlin.de

Table of Contents

1. Experimental Section

1.1. Materials

3,6-dibromo-9-(4-bromophenyl)carbazole (**M1**, 98%), 4-bromocyanobenzene (**M2**, 97%), 5-bromo-2-cyanopyridine (**M3**, 98%), 3-bromopyridine (**M4**, 98%), 5,5'-dibromo-2,2'- bipyridine (**M5**, 98%), 2,4,6-tribromopyridine (**M6**, 97%), 3,5-dibromopyridine (**M7**, 98%), 2,2'-bipyridyl (99%), bis(1,5-cyclooctadiene)nickel(0) (97%), and 1,5-cyclooctadiene (98%) are bought from Tokyo Chemical Industry Co., Ltd and used as received.

1.2. Synthesis of PCZN-1 and modified PCZNs

To a solution of 2,2'-bipyridine (452 mg, 2.9 mmol), bis(1,5-cyclooctadiene)nickel(0) ($Ni(COD)_2$, 800 mg, 2.9 mmol), and 1,5-cyclooctadiene (COD, 0.36 mL, 2.92 mmol) in anhydrous DMF/THF (60 mL/60 mL) add 3,6-dibromo-9-(4-bromophenyl)carbazole (308 mg, 0.64 mmol), and the mixture was stirred at room temperature under argon atmosphere overnight. Then, the mixture was cooled in ice bath, 6 mol/L HCl solution (3 × 40 mL) was added, the resulting mixture was stirred for another 6 h. The precipitate was collected, then washed with methanol (6 × 10 mL) and H_2O (6 × 10 mL), and soxhleted by THF two days, respectively, and dried in vacuum to produce **PCZN-1** as off-white powder (154 mg, 99% yield). To functionalize the **PCZN-1**, 10-50 mol% **M2**, **3**, **4**, **5**, **6** or **7** related to **M1** was introduced to above reaction. To ensure a completed Yamamoto reaction, the amount of corresponding 2,2'-bipyridine, $Ni(COD)_2$, and 1,5-cyclooctadiene catalytic reagents were additionally added.

2. Characterization and measurements

2.1. Structure and morphology characterization

The content of nickel in the final products was simultaneously analyzed by Leeman Labs Prodigy inductively coupled plasma-atomic emission spectrometer (ICP-AES). Fourier transform infrared (FT-IR) spectra were taken on a Varian 640IR spectrometer equipped with an ATR cell. Powder X-ray diffraction (XRD) patterns were obtained on a Bruker D8 Advance diffractometer (40 kV, 30 Ma) using Cu Kα radiation (2θ = 2–80°). Solid-state ^{13}C cross-polarization magic angle spinning nuclear magnetic resonance (CP/MAS NMR) spectra were taken at on a Bruker Avance 400 MHz spectrometer operating at 100.6 MHz. Thermal gravimetric analysis (TGA) was carried out on a TGA 1 instrument from Mettler Toledo in a nitrogen atmosphere in the temperature range 30–1000 °C (heating rate 10 °C/min). Scanning electron microscope (SEM) images were obtained on a Hitachi SU8030 and high-resolution transmission electron microscope (TEM) images were obtained on a TECNAI G2 F20 S-TWIN electron microscope. X-ray photoelectron spectra (XPS) were obtained on a PHI5000 1 Versaprobe-II multifunctional 2 scanning and imaging photoelectron spectrometer equipped with an Al Kα X-ray source.

2.2. Gas adsorption/desorption measurements. Nitrogen adsorption/desorption measurements at 77 K were performed after degassing the samples under high vacuum at 120 °C for 15 hours using an Autosorb IQ_2 from Quantachrome. CO_2 and N_2 adsorption/desorption isotherms at 273 and 298

K as well as H_2 adsorption isotherms at 77 and 87 K were conducted on a Quantachrome Autosorb-1MP instrument after prior degassing under high vacuum (turbomolecular pump) and 120°C. The specific surface areas were calculated by applying the Brunauer-Emmett-Teller (BET) model to adsorption branches of the N_2 isotherms (77.4 K). Pore width analyses were carried out on the basis of N_2 adsorption isotherms using commercialized nonlocal density functional theory (NLDFT) method.

2.3. Isosteric heat of adsorption (Q_{st}) calculations. The isosteric heat of adsorption (Q_{st}) was obtained by Clausius–Clapeyron fitting CO_2 adsorption isotherms measured at 273 and 298 K and H_2 adsorption isotherms measured at 77 and 87 K, respectively.

2.4. Ideal adsorbed solution theory (IAST) selectivity calculations. The IAST calculations were carried out for binary mixture containing 15/85 (v/v) CO_2 and N_2. Pure component gas adsorption isotherms of **PCZN-1**, **5**, **8** and **10** were fitted using the nonlinear regression tool within the OriginPro software (version 2016). The standard Langmuir model was used for N_2 adsorption isotherms fitting, dual-site Langmuir model was used for CO_2 adsorption isotherms fitting as it gives better simulations within the range of interest. The used equations are given below:

$V_{ads} = (q*a*p/(1+a*p))$ (Standard Langmuir model)

$V_{ads} = (q*a*p/(1+a*p))+(u*b*p/(1+b*p))$ (Dual-site Langmuir model)

where p is the pressure given in mmHg, V_{ads} is the adsorbed amount of gas in cm³/g STP, a and b are Langmuir-type affinity constants, q and u represent the Langmuir-type adsorption capacity:

Dual-site Langmuir model fit parameters of the CO_2 adsorption/desorption data at 298 K:

Polymer	q	a	u	b	Error (R^2)
PCZN-1	9.0177	2.94E-3	237.5718	1.61517E-4	0.99999
PCZN-5	9.74421	3.23E-3	192.45983	1.69782E-4	0.99961
PCZN-8	19.39891	2.19E-3	907.14855	3.99902E-5	0.99989
PCZN-10	13.87014	3.8E-3	900.43033	2.05938E-5	0.99977

Standard Langmuir model fit parameters of the N_2 adsorption/desorption data at 298 K:

Polymer	q	a	Error (R^2)
PCZN-1	32.20538	1.75015E-5	0.99619
PCZN-5	1670.90572	2.09565E-6	0.99753
PCZN-8	1197.59338	4.40884E-6	0.99911
PCZN-10	1047.6428	2.66882E-6	0.99825

The pure-component isotherm fitting parameters obtained above were then applied for IAST binary-gas adsorption selectivity (α) calculations based on the equation given below:

$$\alpha = \frac{x_{CO_2}/x_{N_2}}{y_{CO_2}/y_{N_2}}$$

where x represents the amount adsorbed from the binary gas phase, and y represents gas phase composition (i.e. 15/85, v/v). The x values were determined using a Newton-Raphson method implemented within an *octave* (open source software) script.

3. Supplementary Figures

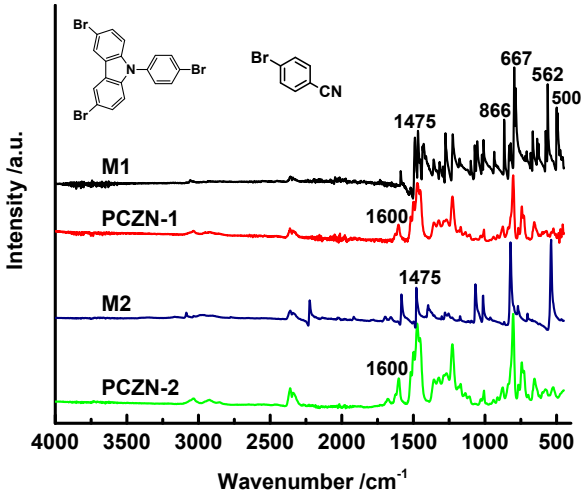

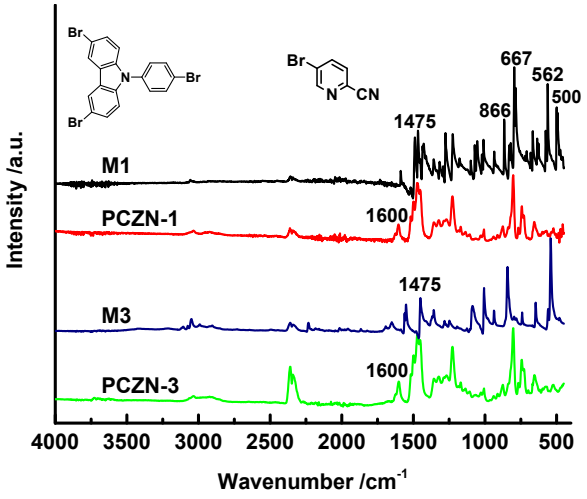

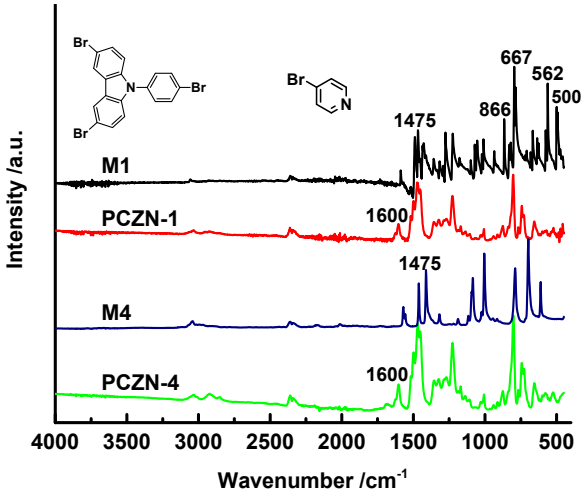
Br
N
Br
Br
Br
N
667
562
500
866
1475
M1
PCZN-1
1600
1475
M4
PCZN-4
1600
Intensity /a.u.
4000 3500 3000 2500 2000 1500 1000 500
Wavenumber /cm-1

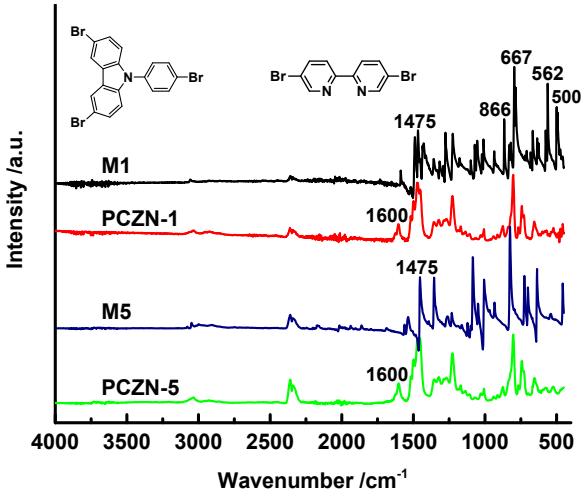
Br
N
Br
Br
Br
N
N
Br
667
562
500
866
1475
M1
PCZN-1
1600
1475
M5
PCZN-5
1600
Intensity /a.u.
4000 3500 3000 2500 2000 1500 1000 500
Wavenumber /cm-1

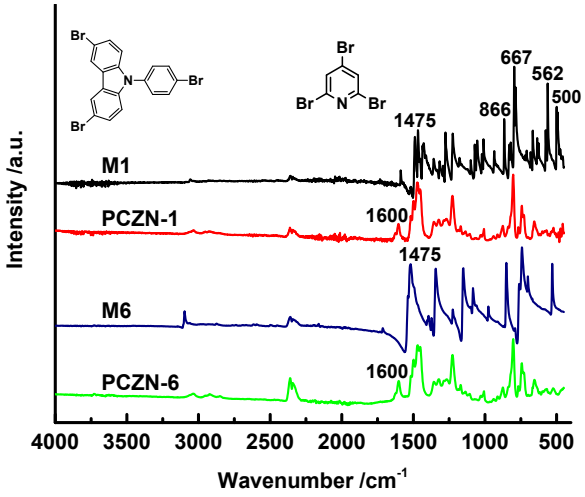
Br
N
Br
Br
Br
Br
N
Br
667
562
500
866
1475
M1
PCZN-1
1600
1475
M6
PCZN-6
1600
Intensity /a.u.
4000 3500 3000 2500 2000 1500 1000 500
Wavenumber /cm-1

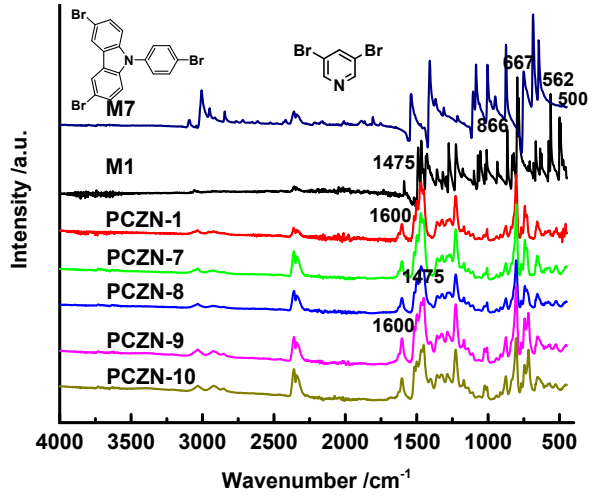

Figure S1 FT-IR spectra of **M1-7** and PCZNs (**1-10**).

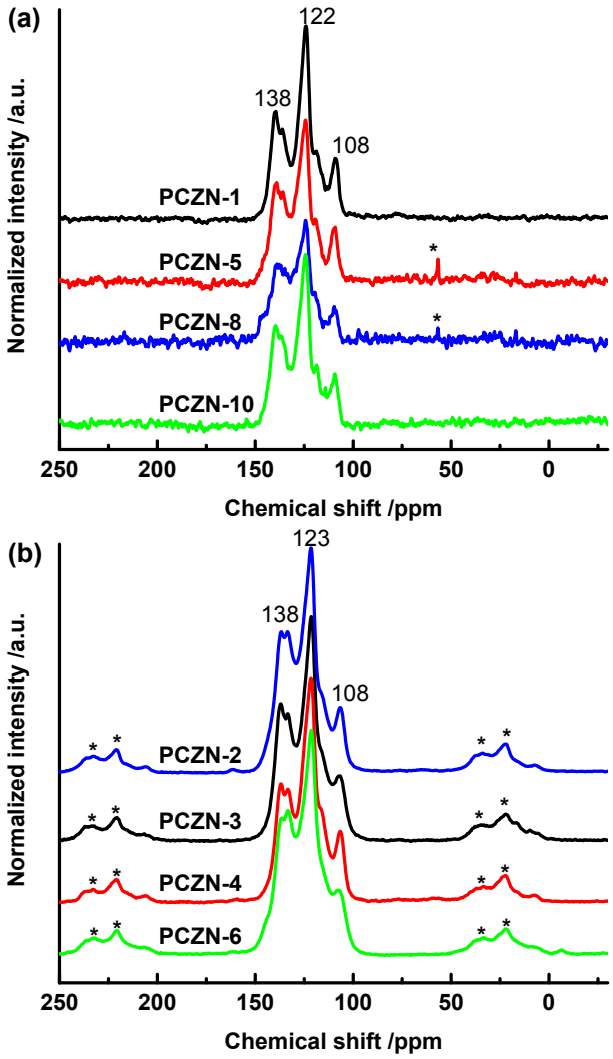

Figure S2 ^{13}C CP/MAS NMR of PCZNs (asterisk mark spinning side bands).

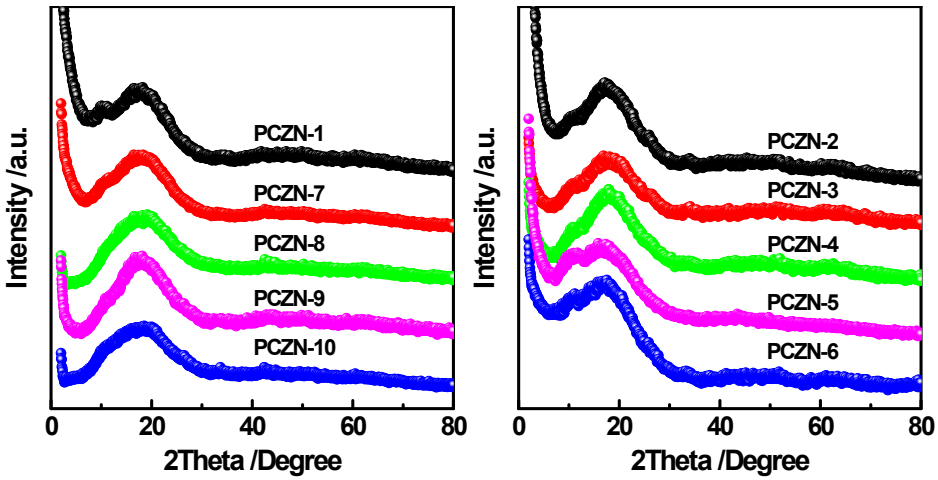

Figure S3 XRD spectra of PCZNs.

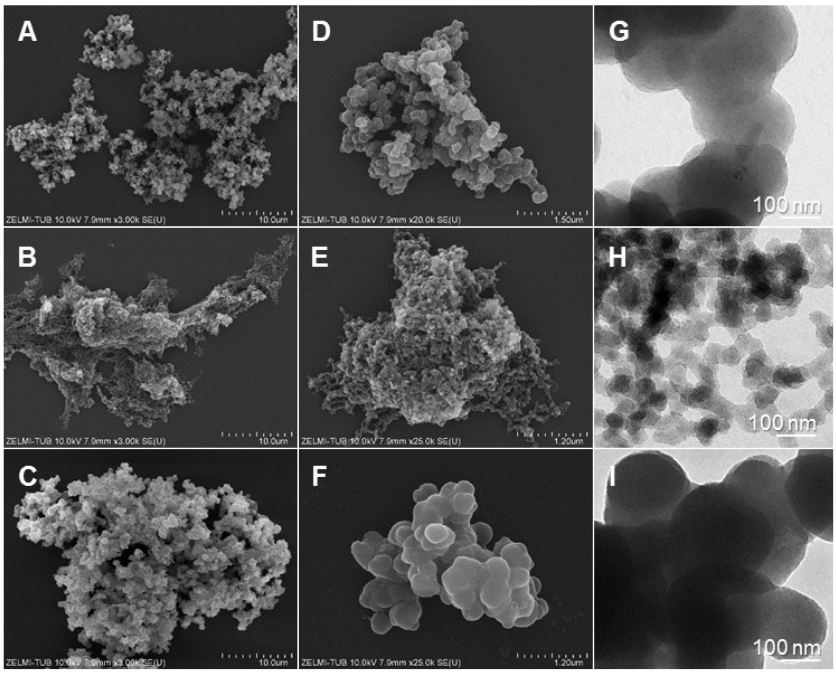

Figure S4 SEM (A-F) and TEM (G-H) images of polycarbazole synthesized with different functional groups: (A,D,G) **PCZN-3**, (B,E,H) **PCZN-5**, and (C,F,I) **PCZN-6**.

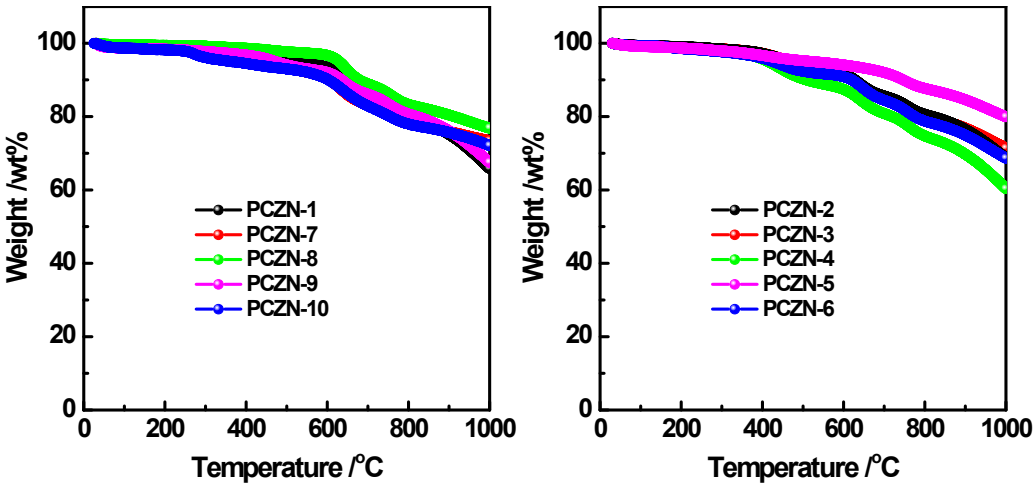

Figure S5 TGA scans of PCZNs in N_2.

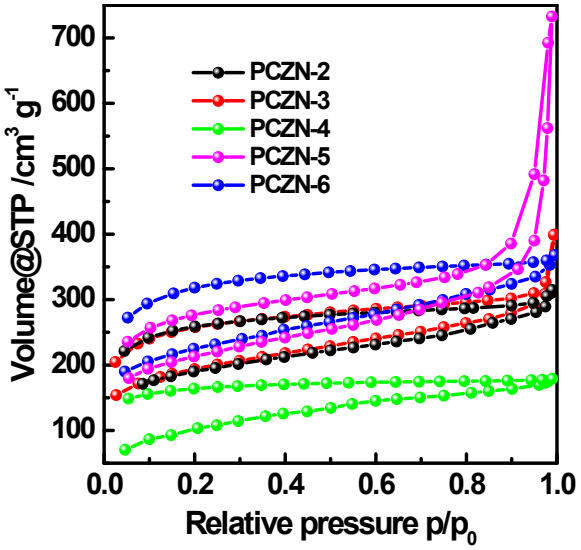

Figure S6 N_2 adsorption/desorption isotherms of **PCZN-2**, **3**, **4**, **5** and **6**.

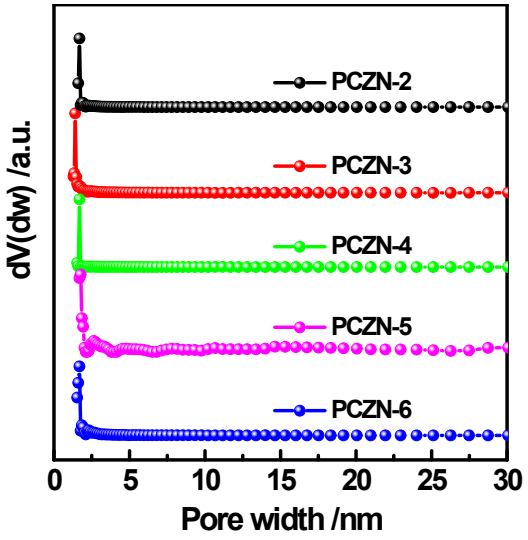

Figure S7 NLDFT pore size distributions of **PCZN-2**,**3**,**4**, **5**, and **6**.

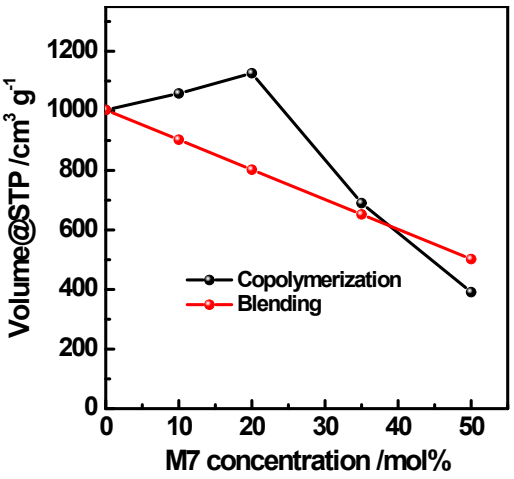

Figure S8 Surface area changes of PCZNs with the introduction of second monomer **M7**.

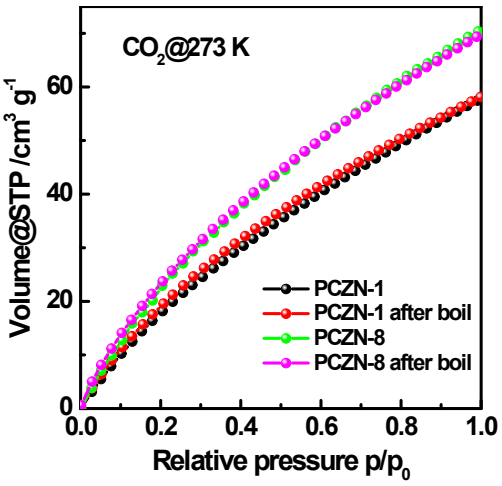

Figure S9 CO_2 adsorption isotherms of **PCZN-1** and **PCZN-8** upon water boiling overnight.

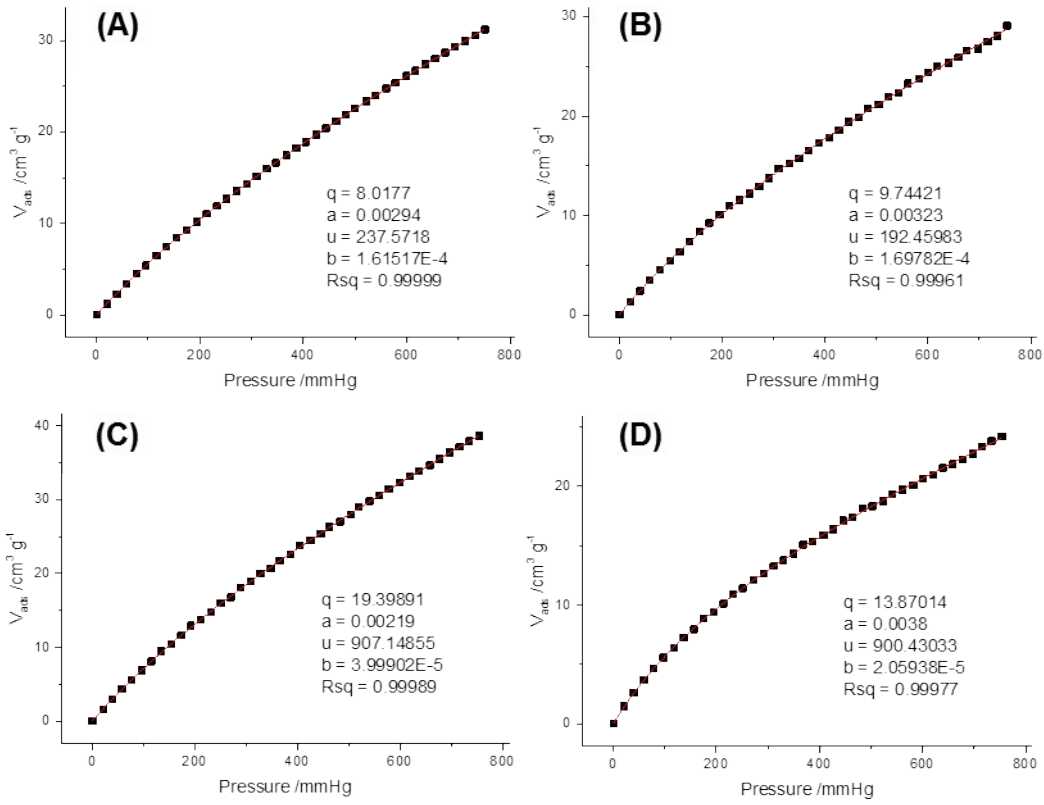

Figure S10 Dual-site Langmuir model fittings of CO_2 isotherms of PCZNs: (A) **PCZN-1**, (B) **PCZN-5**, (C) **PCZN-8** and (D) **PCZN-10** at 298 K.

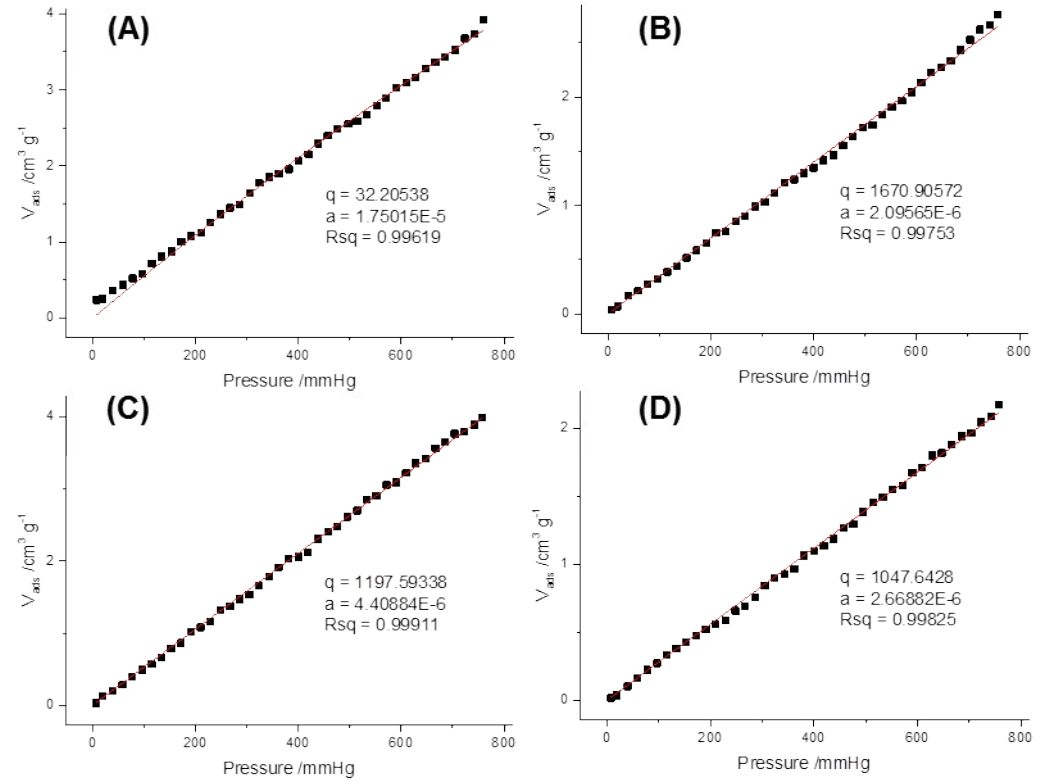

Figure S11 Single-site Langmuir model fittings of N_2 isotherms of PCZNs: (A) **PCZN-1**, (B)

PCZN-5, (C) **PCZN-8** and (D) **PCZN-10** at 298 K.

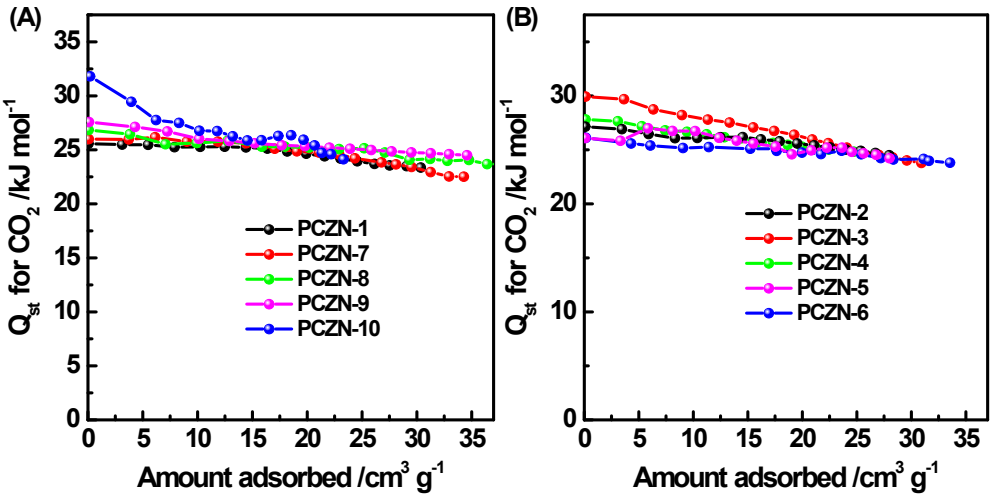

Figure S12 Q_{st} of CO_2 adsorptions of PCZNs.

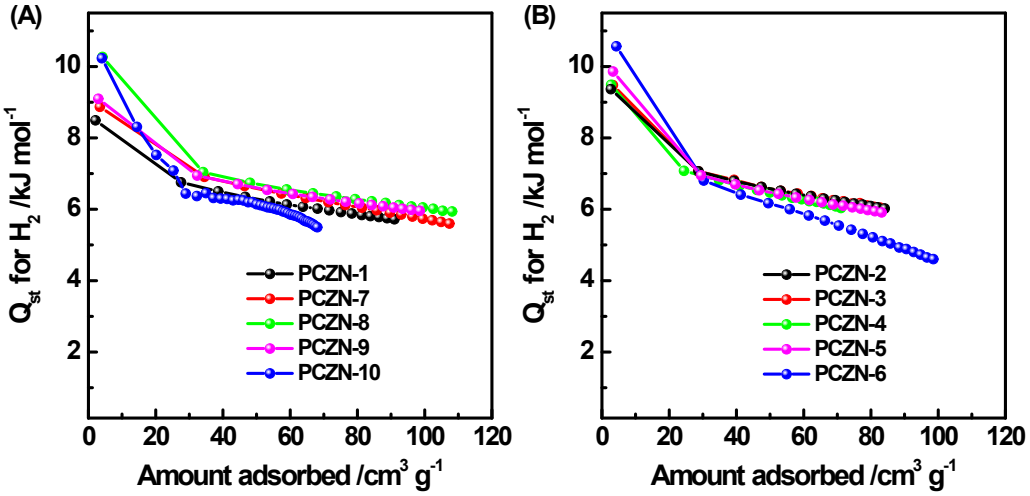

Figure S13 Q_{st} of H_2 adsorptions of PCZNs.